ISSN: 0975 -8542

Journal of Global Pharma Technology

Available Online at: www.jgpt.co.in

RESEARCH ARTICLE

Reduce Graphene Decorated with Iron Oxide/ Polymer Composite for Photo-Fenton Pollutants Dye Degradation

Sara Abdul Karim Dawai*, Khulood A. Al-Saade

Department of Chemistry, College of Science, University of Baghdad Iraq.

***Corresponding Author: Sara Abdul Karim Dawai**

Abstract

The treatment processes for industrial wastewater contains organic pollutants and removal of heavy metal ions remain challenging. In this work, photo Fenton reaction activity was used to degrade the organic pollutants by functional composite hydrogel. The hydrogel is made up of Fe_3O_4 particles, reduced graphene oxide (RGO) and polyacrylamide (PAM). It is prepared from rGO/Fe_3O_4 and by precipitation method, GO has been prepared from graphite by Hummers method. And exhibits the outstanding mechanical strength, Photo-Fenton activity by different decomposition data that were affected differently; pH, H_2O_2 concentration, dye concentration, temperature, irradiation time. The morphology of the composite and the average diameter was studied by Atomic Force Microscopy (AFM). The degradation of M.B dye by Fe_3O_4/rGO/PAM hydrogel composite was reached to 100% after 60 min under UV irradiation. Meanwhile, COD (Chemical Oxygen Demand) decreased to 21 mg/l after one hour's visible irradiation and became low (under range) after 2 hours. This study provides a new pathway to process the industrial wastewater of high consistence and difficult decomposition.

Keywords: *Photo- Fenton reaction, RGO/Fe_3O_4/PAM composite, Methylene Blue, COD.*

Introduction

An advanced oxidation technology include the traditional Fenton reaction which is used for wastewater treatment, the reaction involves a mixture of ferrous iron (Fe^{2+}) and hydrogen peroxide (H_2O_2) in an acidic solution to generate hydroxyl radical (·OH) [1]. Homogeneous Fenton reactions have several disadvantages, such as an acidic pH, low efficiency utilization of H_2O_2 and the generation of sludge [2, 3], these disadvantages restrict its further application. Furthermore, large amounts of Fe^{2+} are required with a large H_2O_2-Fe^{2+} molar ratio, [4, 5] which increases the consumption of reagents. The heterogeneous Fenton reaction uses solid, iron-containing compounds or solid materials rich in iron, such as Fe_3O_4 [6, 7], Fe_2O_3 [8], FEOOH [9], and clay [10], mesoporous silica [11] and activated carbon [12] supported iron-containing compounds, for the degradation of organic pollutants. Comparatively, the heterogeneous Fenton reactions are an effective oxidative technology used to degrade organic pollutants that can efficiently promote H_2O_2 conversion with minimal decomposition, less iron leaching at different pH values and easy separation from solution for cyclic utilization, which are favorable for practical applications. However, most iron-containing catalysts are not feasible and increase iron leaching after cyclic utilization several times because of the weak interaction between the iron catalyst and the carrier materials, which may result in the stability of catalyst and weakened activity. Graphene has been verified as a promising catalyst backup due to its singular physical properties, such as a high electric potential density, electron mobility, and optical absorption [13, 15]. These potential attributes have often been applied in different applications, such as electronics, batteries, sensors and composite materials. there was much attendance has been driven to prepare the hydrogels with superior mechanical properties [16] Commonly there are three types of recipes to prepare the hydrogel with high strength included a topological gel [17], a double network gel [18] and a composite gel [19], among of them composite gels are considered to increase the mechanical properties of hydrogel for

instance the composite gels with a unique organic inorganic network structure would have the extraordinary mechanical properties [20].

Nowadays, graphene oxide (GO) has been no doubt one of the important research topic among chemists, ascribed to low cost for mass production and good dispersibility in water [21, 23]. Meanwhile, its abundant oxygen-containing groups, i.e. carboxyl groups, hydroxyl and epoxide make it favorable elects for improving the mechanical strength of the polymeric hydrogels. PAM is a polymer that is water soluble and widely used in industrial water treatment, and it is treated as non-toxic economic and efficient has undoubtedly of great potential application prospect [24]. Polyacrylamide (PAM) is consisting of amide side groups which are useful for the adsorption of heavy metal ion. Although GO/ Fe_3O_4 based hydrogels have been reported Fe_3O_4/rGO/ PAM hydrogel is much more efficient to adsorb heavy metals This is because of the chemical adsorption ascribed to the metal NH_2 complex [25].

Experimental Part

Determination of Maximum Absorption (λ max)

The wavelength value of M.B absorption is 650 nm was used to estimating its quantity as shown in Figure (1).

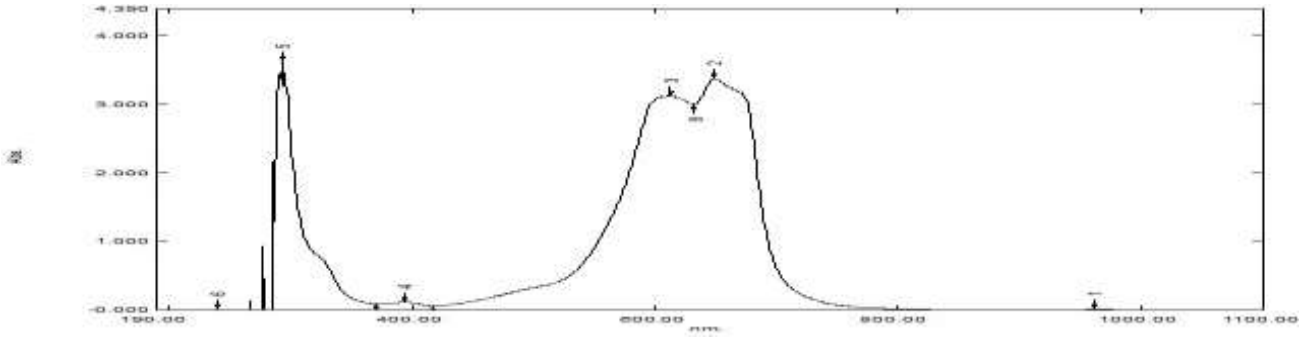

Fig.1: UV-Visible absorption spectrum for methylene blue dye

Figure (2) shows the calibration curve for M.B dye.

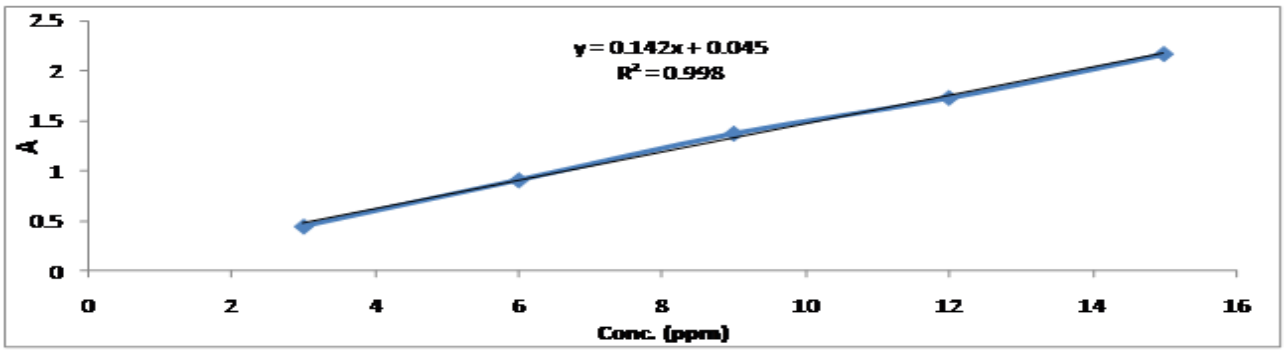

Fig.2: Calibration curve for Methylene blue

Graphene Oxide and Reduced Graphene Oxide Preparation

Graphite 1.0 g was added into 23 mL of concentrated sulphuric acid under stirring at room temperature, then 0.5 g of sodium nitrate was added, and the mixture was cooled to 0°C. Under powerful agitation, 3.0 g of potassium permanganate was added slowly while the temperature of the suspension was kept near 2°C .The reaction mixture was transferred to a water bath at a temperature of 35°C and stirred for 30 min. Then, 50 mL of deionized water DI was added, and the solution was stirred for 15 min at 90°C. Additional 166 mL of water was added and followed by a slow addition of 5 mL of hydrogen peroxide 30%, turning the color of the solution from yellow to dark brown. The mixture was filtered and rinsed with 85 mL of 4% HCl aqueous solution followed by washing with 65 mL of distilled water to remove the acid, then oxidation product washed until the pH reached 6, then filtered and dried. Figure (3) and Figure (4) show The FTIR spectrum of graphene oxide produced by hammers method and The FTIR spectrum of reduced graphene oxide respectively.

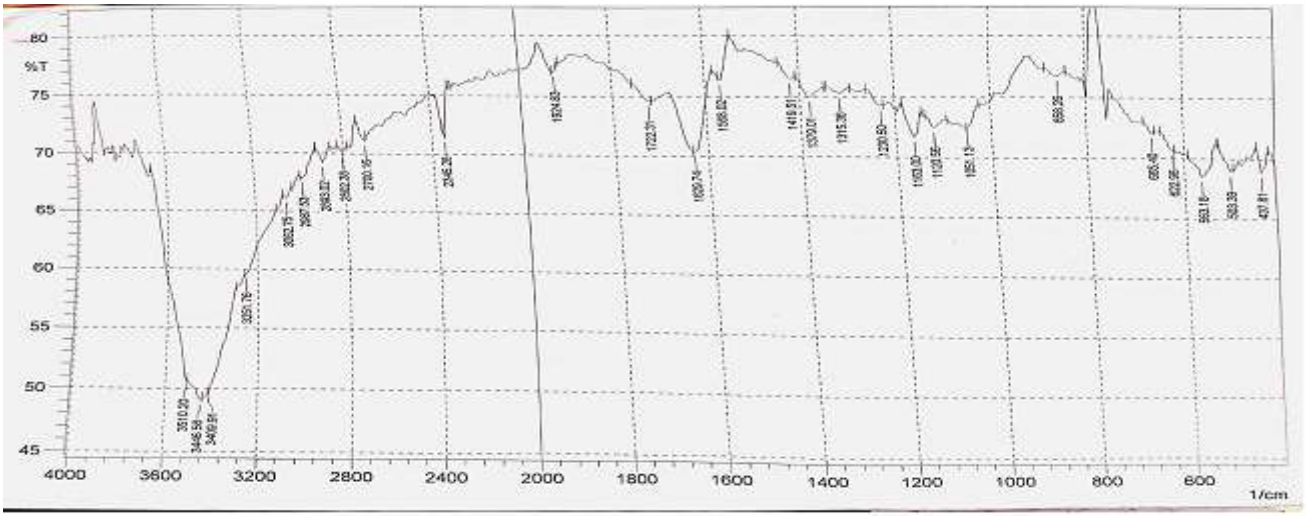

Fig. 3: The FTIR spectrum of graphene oxide produced by hammers method

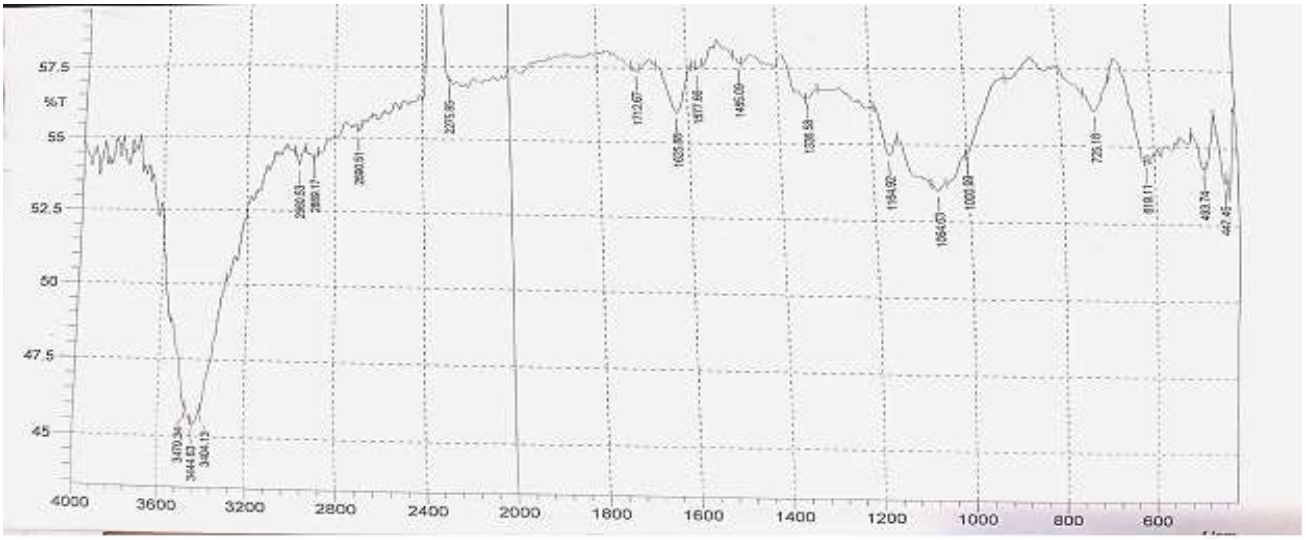

Fig. 4: The FTIR spectrum of reduced graphene oxide

Preparation of rGO/Fe_3O_4 composite

0.2 g GO was added into 150 mL deionized water and underwent the ultrasonic treatment for complete exfoliation of GO. Then, keeping the ultrasound on, 6.5 g of $FeSO_4 \cdot 7H_2O$ was added into the above GO solution. After $FeSO_4 \cdot 7H_2O$ was completely dissolved, the mixed solution was transferred and heated in a water-bath pot to 95°C with continuous mechanical stirring. Subsequently, 80 mL mixed solution of 5.88 g NaOH and 2.94 g $NaNO_3$ was added dropwise and then the obtained black suspension solution was kept at 95°C for 2 h. After being cooled to room temperature. The precipitate was separated by a magnet and alternately washed with anhydrous alcohol and deionized water until the filtrate reached neutral. After being dried at 60°C overnight.

Preparation of rGO/Fe_3O_4/PAM

The rGO/Fe_3O_4/PAM was synthesized by using a simple solvothermal method.

The PAM 0.05g was dissolved in distills water 50 ml by stirred. Farther, at room temperature, rGO/Fe_3O_4 1g was dissolved in PAM solution and stirred for 2 hours. Subsequently, the resultant composite was dried at 80° C in oven for 12 hours.

Preparation of Photocell

Stainless steel pipe with 1cm diameter and 15 cm length Figure (5) was supplied with a copper coil surrounded by the external cell by drop surface and attached to them water bath. Control the temperature of the reactor and lamp solution. The internal cellular surface was first treated with concentrated HF acid to make the inner surface rough and able to capture the casing, and secondly the cell was fully with GO/ Fe_3O_4/PAM composite for 10 minutes to allow the formation of a stable layer, and then release the suspension from the reactor. The photo reactor displays to 500°C in the inner reactor surface to make the catalytic layer more stable as a coating.

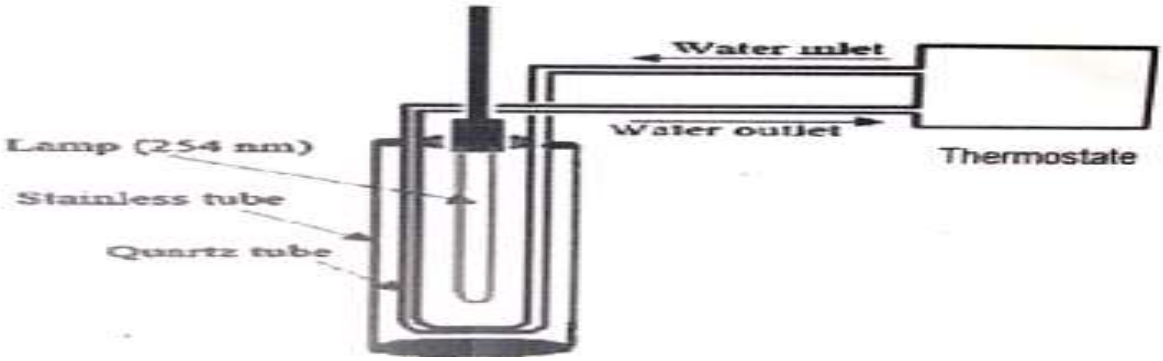

Fig. 5: complete system set up for photo degradation

Result and Discussion

Atomic Force Microscope

The AFM analysis provides the measurements of average grain size and the granularity cumulating distribution for rGO/Fe_3O_4 and rGO/Fe_3O_4/PAM composites.

The average diameter is 206.97 nm and 297.85 nm for rGO/Fe_3O_4 and rGO /Fe_3O_4/PAM composites respectively. Figure (6) shows the Atomic microscopy image for A) rGO/Fe_3O_4 composite. B) rGO/Fe_3O_4/PAM composite.

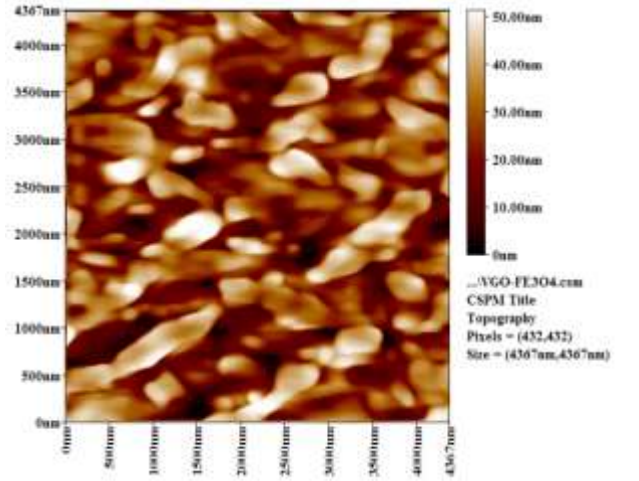

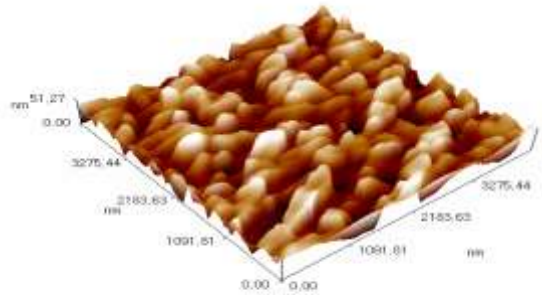

A

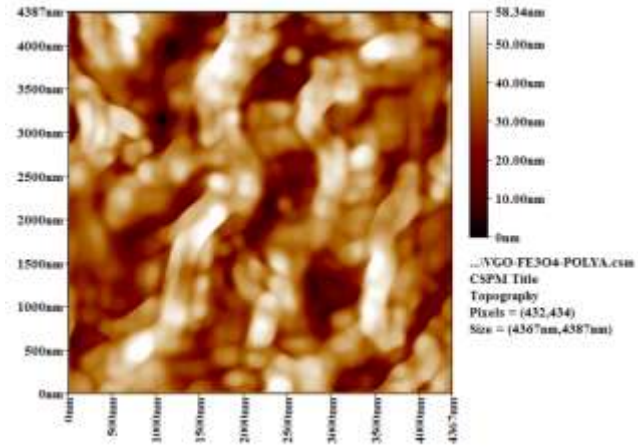

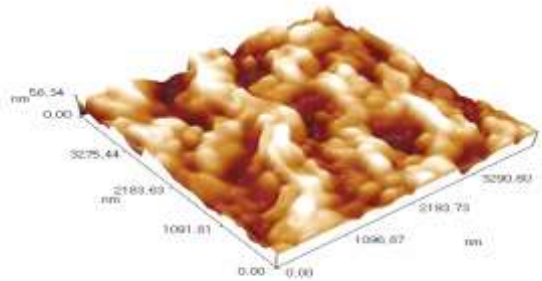

B

Fig. 6: Atomic microscopy image of: A) rGO/Fe_3O_4, B) rGO/Fe_3O_4/PAM

Effect of Fenton reagent

The effect of Fenton on percentage degradation (%deg) of M.B dye using rGO alone and rGO/PAM composite with and without Fenton reagent were studied at pH=7, temperature 298K with H_2O_2 concentration $5*10^{-3}$ M after 60 min, the result shows that the existence of Fenton reagent increases degradation of M.B. as shown in Figure (7).

Effect of PAM Concentration

The effect of PAM concentration on %deg of M.B dye using rGO/Fe_3O_4/PAM composite on M.B %deg was investigated for three different weights (0.01, 0.05, 0.1) g which were show in Figures (8) a, b, c at the following conditions pH=7, H_2O_2 concentration $5*10^{-3}$ M and 298K and the result in Figure (9) show that the best %deg of M.B. was by using 0.05g PAM.

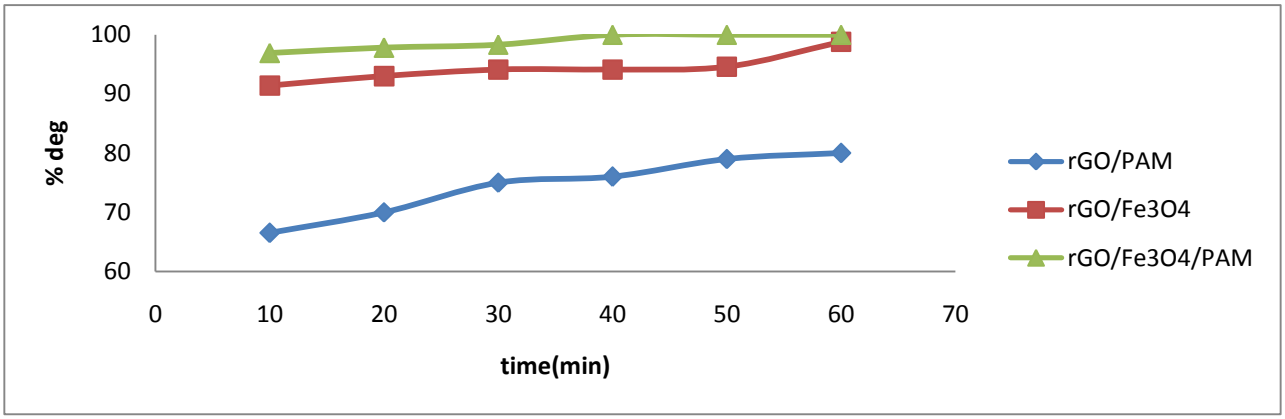

Fig. 7: variation of degradation for (3 ppm) M.B with Fenton at 298K, pH=7, $5*10^{-3}$ H_2O_2 concentration

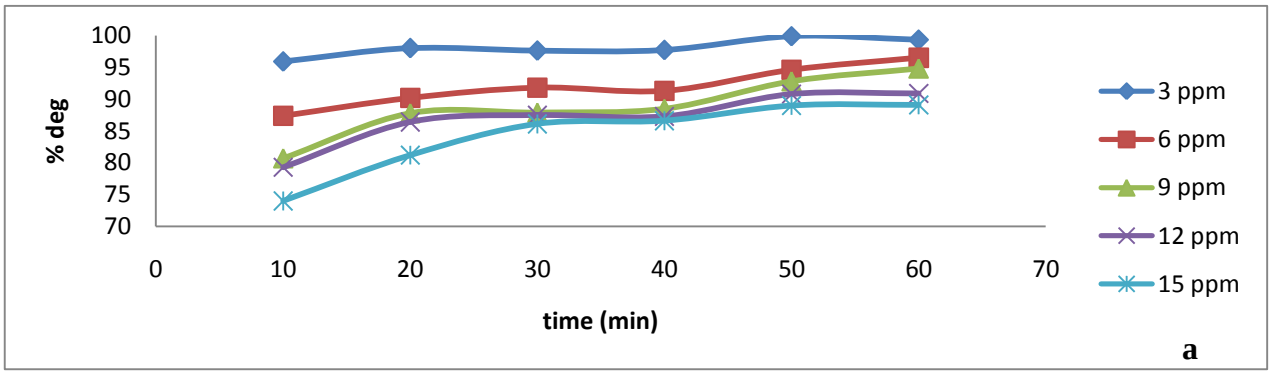

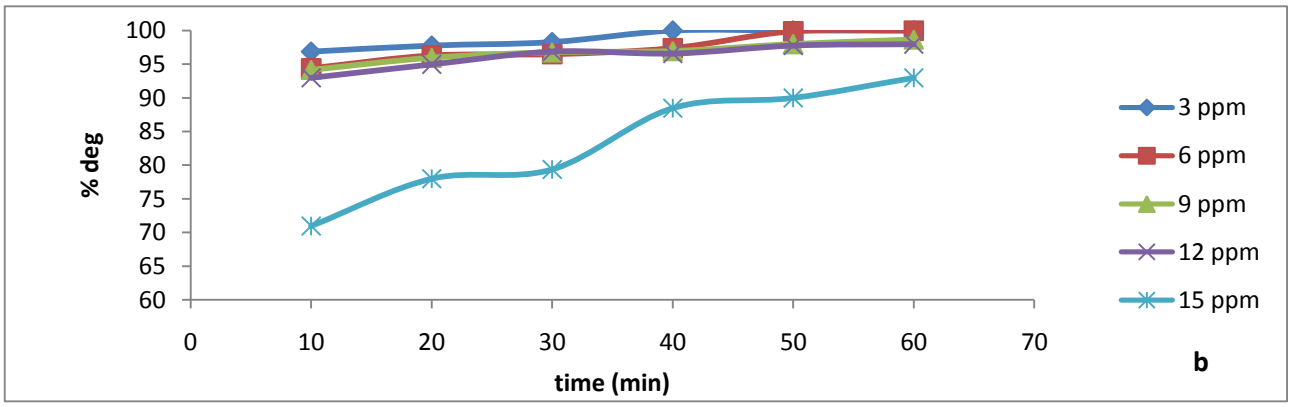

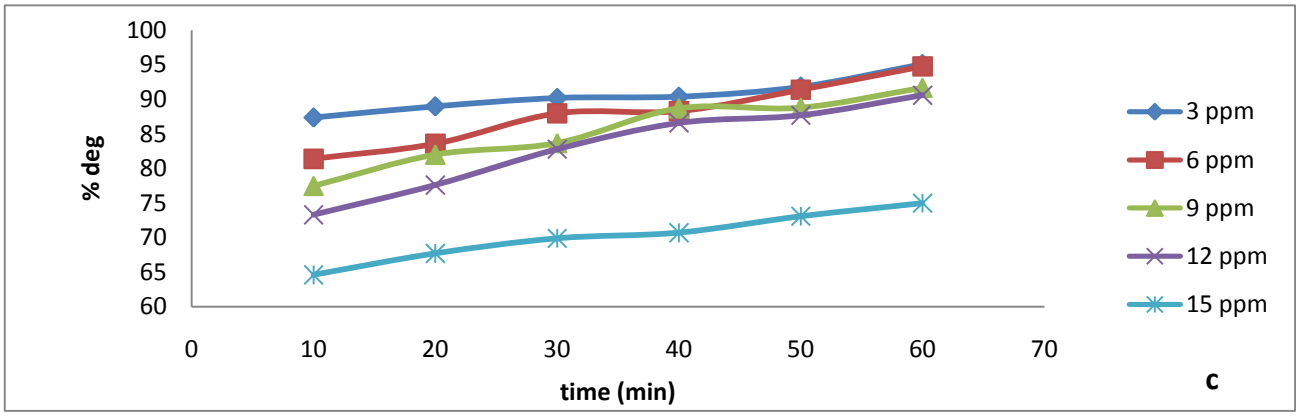

Fig. 8: Variation of %deg. With time for different concentration of M.B by using a) rGO/Fe_3O_4/(0.01)PAM, b) rGO/Fe_3O_4/(0.05)PAM, c) rGO/Fe_3O_4/(0.1)PAM composites

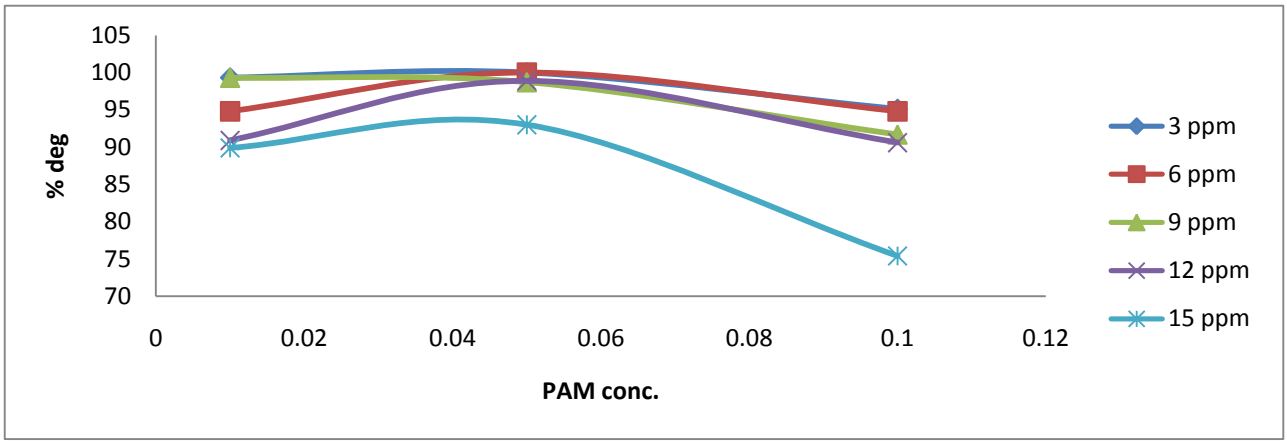

Fig. 9: Effect of PAM concentration variation for different M.B concentration on %deg. after 60 min, at temp. 298K, pH=7 and H_2O_2= 5*10^{-3} M

Effect of Initial Concentration

To study the effect of initial concentration of dye on the degradation efficiency, the experiments were used different initial concentration (3-35) ppm at pH=7, temperature 298K and 5*10^{-3} M H_2O_2 + catalyst (rGO /Fe_3O_4 or rGO/ Fe_3O_4/ PAM composites) after 60 min. as shown in Fig.10 (a), (b).

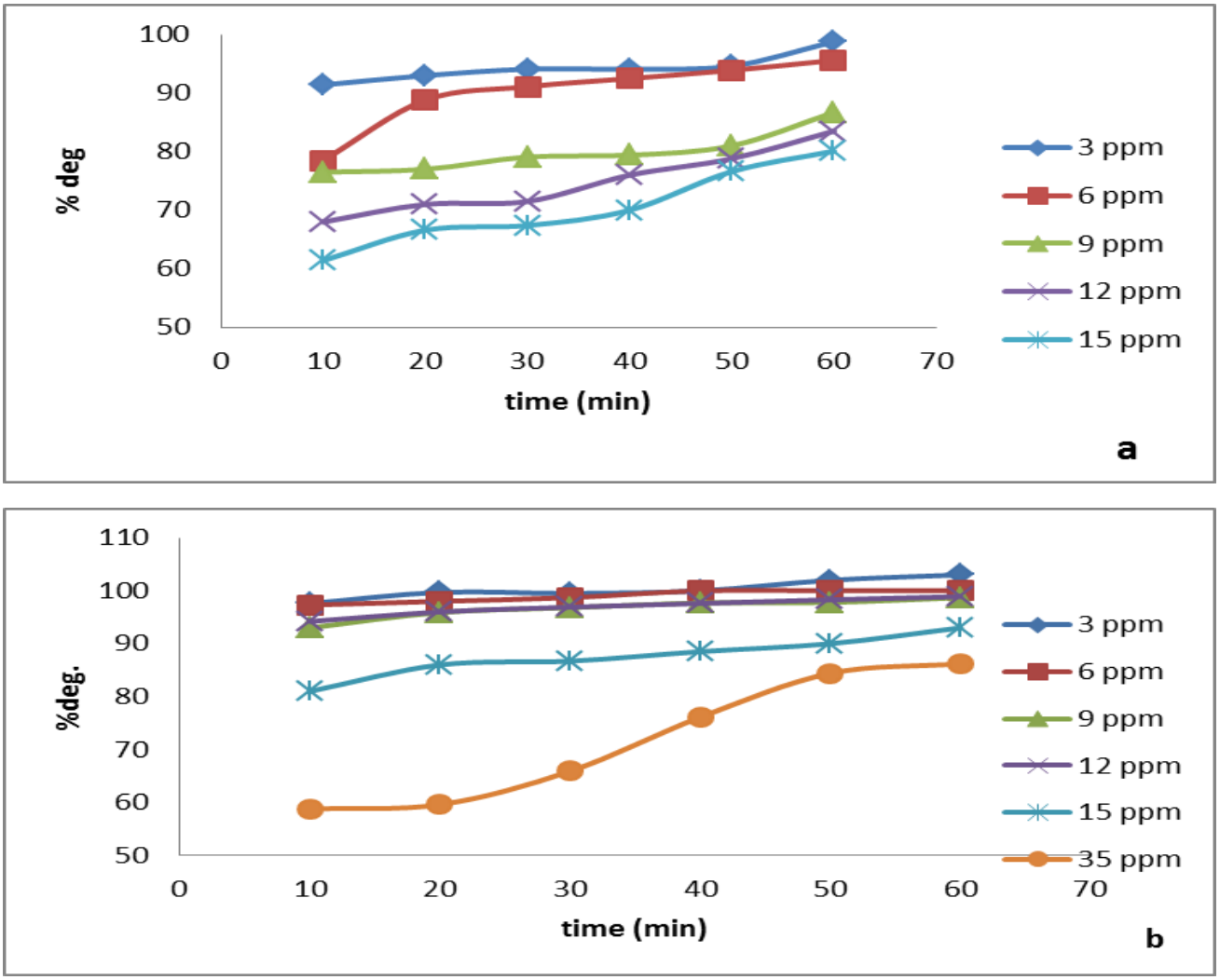

Fig. 10: variation of (%deg) with time for different M.B concentration at 298K, pH=7 and H_2O2 5*10^{-3} M bya) rGO/ Fe_3O_4, b) rGO/Fe_3O_4/PAM catalyst

Effect of H_2O_2 Concentration

The effect of H_2O_2 concentration on the M.B dye degradation at temperature 289K, pH=7, after 30 min in presence of catalyst rGO/Fe_3O_4/PAM composite were studies , the %deg increase with H_2O_2 concentration increased which is shown in Figure (11).

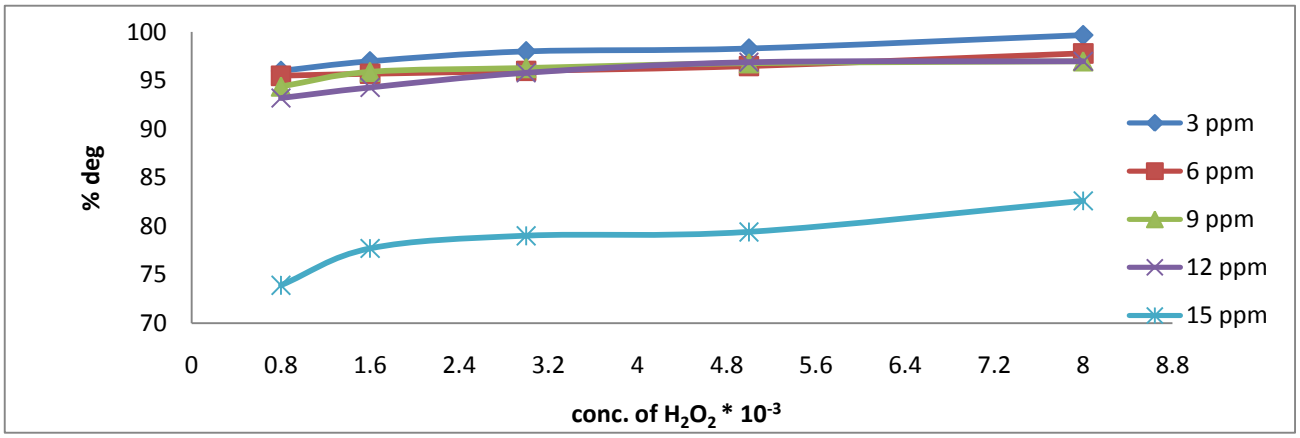

Fig. 11: Effect of varying H_2O_2 concentration for different M.B concentration after 30 min, at 298K, pH=7 on rGO/Fe_3O_4/PAM composite catalyst

Effect of pH on Degradation Process

The effect of pH on the degradation of 15 ppm M.B after 30 min in the presence of rGO/Fe_3O_4/PAM composite and H_2O_2 (0.005M) were shown in the Figure (12). The photolysis reaction was also performed under pH conditions, modified with HCl and NaOH, while composites retained constant amounts on dye solutions.

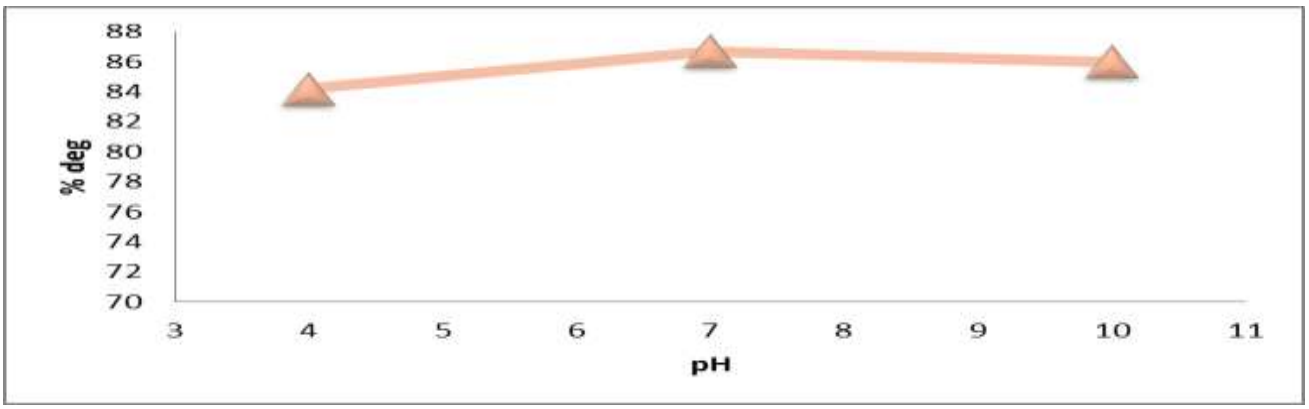

Fig 12: variation of 15 ppm M.B %deg with different pH by rGO/Fe_3O_4/PAM composite and 0.005M H_2O_2

Effect of Temperature

The effect of temperature on (15 ppm) M.B %deg by rGO/Fe_3O_4/PAM composite was investigated in four different temperature (298, 308, 318 and 328)K at pH=7. The result in Figure (13) shows that, the degradation of M.B increased with temperature increased.

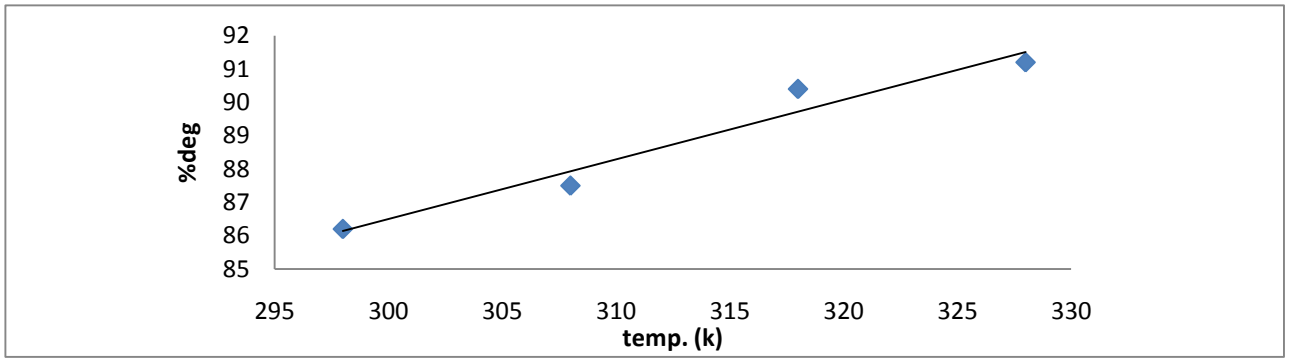

Fig 13: Variation of 15 ppm M.B %deg by rGO/Fe_3O_4/PAM composite with different temperature

Kinetic Degradation Study

The first order equation (1) applied to degradation reaction of 15 ppm M.B and H_2O_2 concentration 0.005 M by using rGO/Fe_3O_4/PAM composite:

$$\mathbf{Ln\ Ce = Ln\ C_0 - Kt} \qquad (1)$$

Where: C_0: initial concentration of M.B, Ce: concentration of M.B after exposing to UV at timet.Fig14 shows the linear relations between Ln Ce and time for 15 ppm M.B dye degradation at four temperatures by three composites

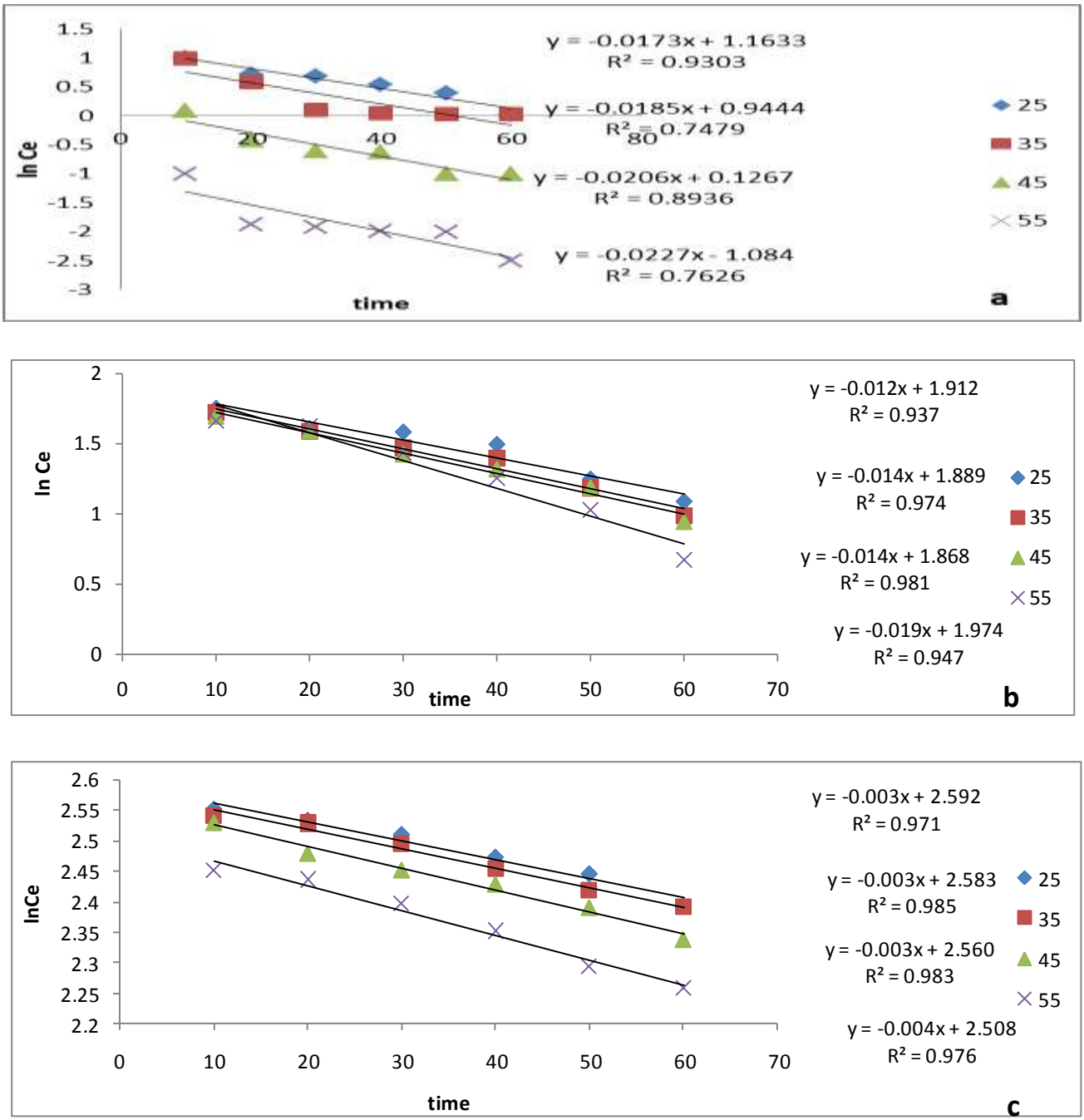

Fig. 14: LnCe V.S time for the degradation of 15 ppm M.B at four temperatures by using three catalysts: a) rGO/Fe_3O_4/PAM composite. b) rGO/Fe_3O_4 composite. c) rGO

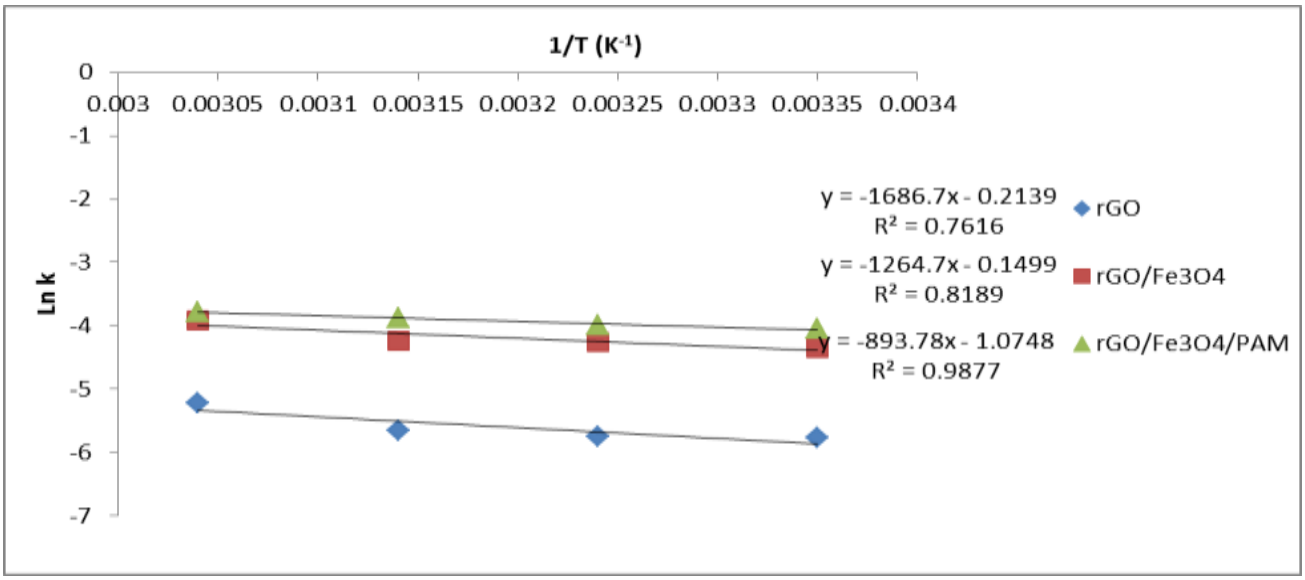

Fig. 15: Arrhenius plots, relation Lnk with 1/T for the10 ppm M.B %deg. rGO/Fe_3O_4/PAM composite, rGO/Fe_3O_4 composite and rGO

Arrhenius equation was applied to calculate kinetic parameter A, Ea. (Figure 15) as following [26]:

$$k = Ae^{-Ea/RT} \quad (2)$$

$$\text{Ln } k = \text{Ln } A - Ea/RT \quad (3)$$

Where T: the absolute temperature (in kelvins), k: the rate constant, Ea is the activation energy for reaction (in k.J mol^{-1}), A is the pre-exponential factor, and R is a global gas constant.

Ea represents the activation (activation energy may also be defined energy as the minimum energy required to start a chemical the reaction) of degradation and A is the pre-of exponential factor in the rate equation. Values of Ea and A are then derived from the slope and the intercept of Ln k versus 1/T plot and represented in Table (1).

Table 1: Kinetic parameter for rGO/Fe_3O_4/PAM composite, rGO/Fe_3O_4 composite and rGO

	T (K)	k/(min)*10^{-3}	Ln k	Ea/kmol^{-1}	A (min^{-1})
rGO/Fe_3O_4/PAM	298	17.3	-4.06	7.418	0.341
	308	18.5	-3.98		
	318	20.6	-3.88		
	328	22.6	-3.78		
rGO/Fe_3O_4	298	12.8	-4.35	10.497	0.860
	308	14.2	-4.25		
	318	14.5	-4.23		
	328	19.8	-3.92		
rGO	298	3.1	-5.77	13.999	0.807
	308	3.2	-5.74		
	318	3.5	-5.65		
	328	4.1	-5.49		

The presence of PAM lead to decrease Ea from13.999 kJ mol^{-1} to 7.148kJmol^{-1}, so the degradation of (15 ppm) M.B dye will be more favorable and more easy

Chemical Oxygen Demand (Cod) Test

COD often is used as a measurement of pollutants in wastewater and natural waters. The result of COD removal was 21 mg/L after 60 min of irradiation time for 3 ppm concentration of M.B at pH=7, temperature 298K and 0.005M H_2O_2 by rGO/Fe_3O_4/PAM composite. After 2h this result decreased to reach to Zero value under the same conditions.

Conclusion

In summary, the Methylene Blue dye degradation capacity on reduced graphene oxide/ Fe_3O_4/ poly acryl amide composite as catalyst which was prepared by precipitation method was studied. The characterization of composite such as average diameter and morphology were achieved by AFM. AFM image detection that the particles size increase after adding PAM to rGO/Fe_3O_4 composite and the efficiency of % degradation for M.B increase. Photo-Fenton process was successfully applied to remove the pollutants dye by rGO/Fe_3O_4/PAM composite as catalyst. 60 minutes was selected as the best irradiation time. The results of pH effect showed that the best degradation of M.B dye on rGO/Fe_3O_4/PAM composite was in Ph=7. Temperature effect results showed that the degradation of M.B dyes on the rGO/Fe_3O_4/PAM composite was increased with increase temperature.

The color was removed completely and the dye converted into organic material then degradation is complete after the dye solution is exposed to irradiation for longer period, (COD test after 2h is low or under range). The kinetic study results indicated that M.B dye degradation on rGO/Fe_3O_4/PAM composite was good construed with the first-order. Finally, it is recommended to apply the used technique (photo Fenton process) as treatment of wastewater containing organic compound.

References

1. Fenton HJH (1894) Oxidation of tartaric acid in presence of iron. J. Chem. Soc., Trans., 65: 899-910.
2. Kremer ML (2003) The Fenton reaction. Dependence of the rate on pH. J. Phys. Chem. A, 107: 1734-1741.
3. Lin SH, Lo CC (1997) Fenton process for treatment of desizing wastewater. Water Res., 31: 2050-2056.
4. Iurascu B, Siminiceanu I, Vione D, Vicente MA, Gild A (2009) Phenol degradation in water through a heterogeneous photo-Fenton process

catalyzed by Fe-treated laponite. Water Res., 43: 1313-1322.

5. Dercova K, Branislav V, Tandlich R, Subova L (1999) Fenton's type reaction in chemical pretreatment of PCBs. Chemosphere, 39: 2621-2628.
6. Gao LZ, Zhuang J, Nie J, Zhang JB, Gu N, Wang TH, Feng J, Yang SL, Perrett S, Yan XY (2007) Intrinsic peroxidase-like activity of ferromagnetic nanoparticles. Nat. Nanotechnol., 2: 577-583.
7. Xu LJ, Wang JL (2012) Fenton-like degradation of 2, 4- dichlorophenol using Fe3O4 magnetic nanometer particles. Appl. Catal., B, 123: 117-126.
8. Guo LQ, Chen F, Fan XQ, Cai WD, Zhang JL (2010) S-doped α-Fe2O3 as a highly active heterogeneous Fenton-like catalyst towards the degradation of acid orange 7 and phenol. Appl. Catal., B, 96: 162-168.
9. Lin SS, Gurol MD (1998) Catalytic decomposition of hydrogen peroxide on iron oxide: kinetics, mechanism, and implications. Environ. Sci. Technol., 32: 1417-1423.
10. Ramirez JH, Costa CA, Madeira LM, Mata G, Vicente MA, Rojas-Cervantes ML, López-Peinado AJ, Martín-Aranda RM (2007) Fenton-like oxidation of Orange II solutions using heterogeneous catalysts based on saponite clay. Appl. Catal., B, 71: 44-56.
11. Coelho JV, Guedes MS, Prado RG, Tronto J, Ardisson JD, Pereira MC, Oliveira LCA (2014) Effect of iron precursor on the Fenton-like activity of Fe2O3/mesoporous silica catalysts prepared under mild conditions. Appl. Catal., B, 144: 792-799.
12. Sun LJ, Yao YY, Wang L, Mao YJ, Huang ZF, Yao DC, Lu WY, Chen WX (2014) Efficient removal of dyes using activated carbon fibers coupled with 8-hydroxyquinoline ferric as a reusable Fenton-like catalyst. Chem. Eng. J., 240: 413-419.
13. Nair RR, Blake P, Grigorenko AN, Novoselov KS, Booth TJ, Stauber T, Peres NMR, Geim A K (2008) Fine structure constant defines visual transparency of graphene. Science, 320: 1308.
14. Moser J, Barreiro A, Bachtold A (2007) Current-induced cleaning of graphene. Appl. Phys. Lett., 91: 163-513.
15. Mayorov AS, Gorbachev RV, Morozov SV, Britnell L, Jalil R, Ponomarenko LA, Blake P, Novoselov KS, Watanabe K, Taniguchi T, Geim AK (2011) Micrometer-scale ballistic transport in encapsulated graphene at room temperature. Nano Lett., 11: 2396-2399.
16. Su DM Yao, Liu J, Zhong Y, Chen X, Shao Z (2017) Enhancing mechanical properties of silk fibroin hydrogel through restricting the growth of ß-sheet domains, ACS Appl. Mater. Interface, 9: 17489-17498.
17. Okumura Y Ito K (2001) The polyrotaxane gel: a topological gel by figure-of-eight crosslinks, Adv. Mater., 13: 485-487.
18. Gong JP (2010) Why are double network hydrogels so tough? Soft Matter, 6: 2583-2590.
19. Haraguchi K, Takehisa T (2002) Nanocomposite hydrogels: a unique organic-inorganic network structure with extraordinary mechanical, optical, and swelling/de-swelling properties, Adv. Mater., 14: 11-20.
20. Hom WL, Bhatia SR (2017) Significant enhancement of elasticity in alginate-clay nanocomposite hydrogels with PEO-PPO-PEO copolymers, Polymer, 109: 170-175.
21. Xing M, Shen F, Qiu, B, Zhang J (2014) Highly-dispersed boron-doped graphene nanosheets loaded with TiO2 nanoparticles for enhancing CO2 photoreduction, Sci. Rep., 4.
22. Qiu B, Xing M, Zhang J (2015) Stöber-like method to synthesize ultra light porous, stretchable Fe2O3/graphene aero gels for excellent performance in photo-Fenton reaction and electrochemical capacitors, J. Mater. Chem. A 3: 12820-12827.
23. Qiu, B Xing, M. Zhang, J. Mesoporous TiO2 nanocrystals grown in situ on grapheme aerogels for high photo catalysis and lithium-ion batteries, J. Am. Chem. Soc. 136 (2014) 5852-5855.
24. Fu F, Wang Q (2011) Removal of heavy metal ions from wastewaters: a review, J. Environ. Manag., 92: 407-418.
25. Zhao, Y. Chen, Y. Li, M. Zhou, S. Xue, A. Xing, W. Adsorption of Hg2+ from aqueous solution onto polyacrylamide/attapulgite, J. Hazard. Mater., 171 (2009) 640-646.
26. Arrhenius S (1889) "Uber Die Dissociationswarme und Den Einfluss Der Temperatur Auf Den Dissociations grad Der Elektrolyte, Zeitschrift fur physikalische', Chemie., 4 (1): 96-116.

